ELSEVIER

Physica B 298 (2001) 573–579

PHYSICA B

www.elsevier.com/locate/physb

Energy relaxation process in a quantum dot studied by DC current and pulse-excited current measurements

Toshimasa Fujisawa[a,*], Yasuhiro Tokura[a], Yoshiro Hirayama[a,b]

[a]NTT Basic Research Laboratories, 3-1 Morinosato-Wakamiya, Atsugi, 243-0198 Kanagawa, Japan
[b]CREST, 4-1-8 Honmachi, Kawaguchi, 331-0012 Saitama, Japan

Abstract

Energy relaxation from an excited to a ground state in a quantum dot is studied by DC current and pulse-excited current measurements. We find that all the excited states can be classified as short-lived or long-lived excited states, although they are too short or too long for us to determine the actual lifetime with our method. The relaxation time is short (less than a few ns) if the transition takes place by means of electron–phonon interaction, while it is very long (more than a few μs) if the transition involves a spin-flip. The crossover between long and short relaxation time is studied at a particular level crossing. © 2001 Elsevier Science B.V. All rights reserved.

PACS: 73.61.Ey; 73.23.Hk; 85.30.Vw

Keywords: Quantum dot; Coulomb blockade; Spin; Energy relaxation

1. Introduction

Electronic quantum dots, in which discrete energy states are filled with a tunable number of electrons, exhibit a variety of orbital effects and spin-related phenomena (For a review see Ref. [1]; and also see Refs. [2,3]). These conventional DC transport studies measured the overlap of the dot state and the reservoir. However, the transitions between these dot states, which are responsible for the coupling to the environment, should strongly reflect the characteristics of the states. Theory predicts that the energy relaxation time of an excited state (ES) in a quantum dot is of the order of nanoseconds if the transition is accompanied by an acoustic phonon emission provided the spin is disregarded [4]. By contrast, it should be extremely long if the transition involves a spin flip [5]. Only a few experimental reports address the relaxation in electronic quantum dots [6,7]. Recently, we have developed a pulse-excitation measurement technique to determine the relaxation time in a quantum dot [8]. In the present paper, we describe in detail our estimation of the relaxation time both from DC current and pulse-excited current measurements. We also focus on the crossover between short and long relaxation time at a specific magnetic field where two ESs cross each other.

*Corresponding author. Tel.: +81-462403449; fax: +81-462404727.

E-mail address: fujisawa@will.brl.ntt.co.jp (T. Fujisawa).

0921-4526/01/$ - see front matter © 2001 Elsevier Science B.V. All rights reserved.
PII: S0921-4526(01)00385-4

2. DC Transport measurement

A quantum dot is fabricated in an AlGaAs/GaAs modulation doped heterostructure by using focused ion beam implantation (dark horizontal lines in SEM image of Fig. 1(a)) and Schottky gates (bright vertical lines separated by 220 nm) [7,9]. We performed all the measurements at a temperature of 150 mK and in a magnetic field applied perpendicular to the substrate. The dot contained about $N \sim 50$ electrons, and showed an addition energy of about 2 meV and single particle energy spacings of 100–300 μeV. We tuned the two gate voltages, V_L and V_R, such that the tunneling rate of the left barrier, Γ_L, was much larger than that of the right barrier, Γ_R. Therefore, the incoming tunnel rate to the dot is larger than the outgoing tunnel rate at a positive bias voltage, $V_b > 0$, (for the polarity defined in Fig. 1(a)), and the reverse at a negative bias voltage. Fig. 1(b) shows typical current through the dot at various V_b. The current increases stepwise when a discrete energy, E_i, enters the transport window (between the left and right

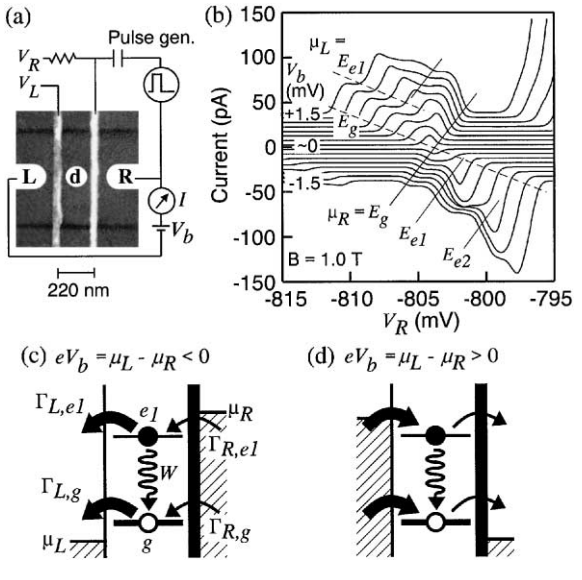

Fig. 1. (a) Schematic setup for the pulse measurements. (b) Single-electron tunneling current at various bias voltages, V_b. Each line is shifted by 5 pA for clarity. (c) and (d) Schematic energy diagrams. (c) is the situation at a negative V_b, where the ground, g, and the first excited state, e_1, are located in the transport window. (d) is the situation at a positive V_b.

Fermi energies, μ_L and μ_R, respectively). E_g, E_{e1}, and E_{e2} are the energies of the GS, g, the first ES, e_1, and the second ES, e_2, respectively. Since the current is limited by the thick barrier on the right, current steps appear at $\mu_R = E_i$ as indicated by solid lines. All the energy states in a quantum dot can be detected in this way, unless the coupling to the leads is too weak. Another type of current step appears at the resonance associated with the thin barrier, $\mu_L = E_i$ (dashed lines), but it appears only for specific ESs; a step is seen at $\mu_L = E_{e1}$ but not at $\mu_L = E_{e2}$ in Fig. 1(b). The qualitative difference can be explained in terms of the different relaxation times as follows.

We consider a simple situation where the GS, g, and the first ES, e_1, are in the transport window (Figs. 1(c) and (d)). Each state ($i = g, e_1$) is coupled to the right and left lead with tunneling rates, $\Gamma_{R,i}$ and $\Gamma_{L,i}$, respectively. We also consider the energy relaxation rate, W, from the ES to the GS. We calculated the current through the dot from the rate equations considering all the processes described by arrows in Figs. 1(c) and (d). For a negative bias voltage (Fig. 1(c)), the rate equations at equilibrium are

$$\frac{d}{dt}\rho_{e1} = \Gamma_{R,e1}(1 - \rho_{e1} - \rho_g) - \Gamma_{L,e1}\rho_{e1} - W\rho_{e1} = 0,$$

$$\frac{d}{dt}\rho_g = \Gamma_{R,g}(1 - \rho_{e1} - \rho_g) - \Gamma_{L,g}\rho_g + W\rho_{e1} = 0, \quad (1)$$

where ρ_g and ρ_{e1} ($0 \leqslant \rho_g, \rho_{e1} \leqslant 1$) are the average electron numbers in the GS and ES, respectively. For the large asymmetric barriers, $\Gamma_{L,g}, \Gamma_{L,e1} \gg \Gamma_{R,g}, \Gamma_{R,e1}$, the total negative current, $I_n = -e(\Gamma_{L,g}\rho_g + \Gamma_{L,e1}\rho_{e1})$, is given by

$$I_n = -e(\Gamma_{R,g} + \Gamma_{R,e1}), \quad (2)$$

which is independent of W. Generally, the saturated current, I_n, is given by the rate $\Gamma_{R,i}$ through the thick barrier to the ith empty state located in the transport window; $I_n = -e\sum\Gamma_{R,i}$. Thus all the energy states in a quantum dot can be detected in this way, unless the coupling to the leads $\Gamma_{R,i}$ is too weak.

We obtained the rate equations for the positive bias voltage (Fig. 1(d)) by exchanging $\Gamma_{L,i}$ and $\Gamma_{R,i}$ in Eq. (1). In this case the positive total current, I_p, is a function of W;

$$I_p = \frac{e\Gamma_{R,g}(\Gamma_{L,g} + \Gamma_{L,e1})(\Gamma_{R,e1} + W)}{\Gamma_{L,g}(\Gamma_{R,e1} + W) + \Gamma_{L,e1}(\Gamma_{R,g} + W)}. \quad (3)$$

In the limit of fast relaxation, $W \gg \Gamma_{R,g}$, $\Gamma_{R,e1}$, the current becomes

$$I_p = e\Gamma_{R,g}, \quad (4)$$

which is identical to the current only through the GS. In the other limit of slow relaxation, $W \ll \Gamma_{R,g}$, $\Gamma_{R,e1}$,

$$I_p = \frac{e\Gamma_{R,g}\Gamma_{R,e1}(\Gamma_{L,g} + \Gamma_{L,e1})}{\Gamma_{L,g}\Gamma_{R,e1} + \Gamma_{L,e1}\Gamma_{R,g}}, \quad (5)$$

which is different from Eq. (4) if $\Gamma_{R,g} \neq \Gamma_{R,e1}$. The current step appears at $\mu_L = E_{e1}$ only when the relaxation rate is not much larger than the tunneling rate.

If more than two ESs are in the transport window, a similar argument can be made by considering W to be the sum of all the relaxation from the ES to any lower lying energy states. For the data in Fig. 1(b), the appearance of a current step at $\mu_L = E_{e1}$ and its disappearance at $\mu_L = E_{e2}$ reflect the difference in relaxation time; i.e., the relaxation from e_1 to g is slow, and the relaxation from e_2 to e_1 or from e_2 to g is fast. Although Eq. (3) is too complicated for us to determine W experimentally from I_p, the appearance or disappearance of the step is a good practical measure of the relaxation time as we described below.

3. Pulse-excited current

We performed pulse excitation measurements, in which we were able to estimate the relaxation time by changing the pulse width. We applied a pulse signal to the right gate in order to modulate the electrostatic potential of the dot (see Fig. 1(a)). Fig. 2(a) shows a pulse waveform with a length $t_p = 10$ ns, which is the shortest pulse we used in this study. During the steady state (low-level) of the pulse, both the ES and the GS are located above μ_L and μ_R for a sufficiently long period to ensure that these states are completely empty (Fig. 2(b)). The positive pulse pushes down the potential of the dot by 100–800 μeV, which is smaller than the addition energy of the dot. Thus, the GS and the ES cannot be simultaneously occupied due to Coulomb blockade. If the potential is pushed down such that only the ES is located in the transport window (see Fig. 2(c)), non-equilibrium transport through the ES continues until the GS becomes occupied. First, an electron tunnels into the dot either to the ES or to the GS with a probability ratio $\Gamma_{L,e1}:\Gamma_{L,g}$. If an electron is injected into the ES, it can relax to the GS, or tunnel to the right lead to give a net current. The transport is blocked once the GS is occupied. We chose asymmetric barriers, $\Gamma_L \gg \Gamma_R$, such that an electron stays in the ES for a long time. Thus, the decay time of the non-equilibrium transport should reflect the energy relaxation rate, W. The pulse ($t_p = 10$ ns–10 μs) is repeated at a period, t_r, and the average current is measured.

Fig. 2(d) shows the pulse-excited current measured at a small bias voltage ($V_b = 0.1$ mV). The bias voltage should be large enough to saturate the current,[1] but a smaller voltage is desirable for a better energy resolution. The application of the pulse signal splits the current peak into two peaks, which correspond to the tunneling through the GS during the pulse (labeled g in the figure) or after the pulse (the rightmost peak). An extra peak (labeled e_1), which is the non-equilibrium current through the lowest ES, appears in-between the two split peaks. The peak spacing between g and e_1 is independent of the pulse amplitude, and the corresponding energy spacing agrees well with that obtained from normal DC measurements.

We obtained the average number of tunneling electrons through the GS, $\langle n_g \rangle$, and through the ES, $\langle n_e \rangle$, per pulse from It_r/e for each peak current I, and plotted them in Fig. 2(e) for the same condition of Fig. 2(d), and in Fig. 2(f) for less-transparent

[1] If the bias voltage is in the linear conductance regime, tunneling back from the ES to the left lead enhances the trapping of an electron in the GS regardless of the relaxation. We see that the non-equilibrium tunneling current is super-linearly dependent on V_b.

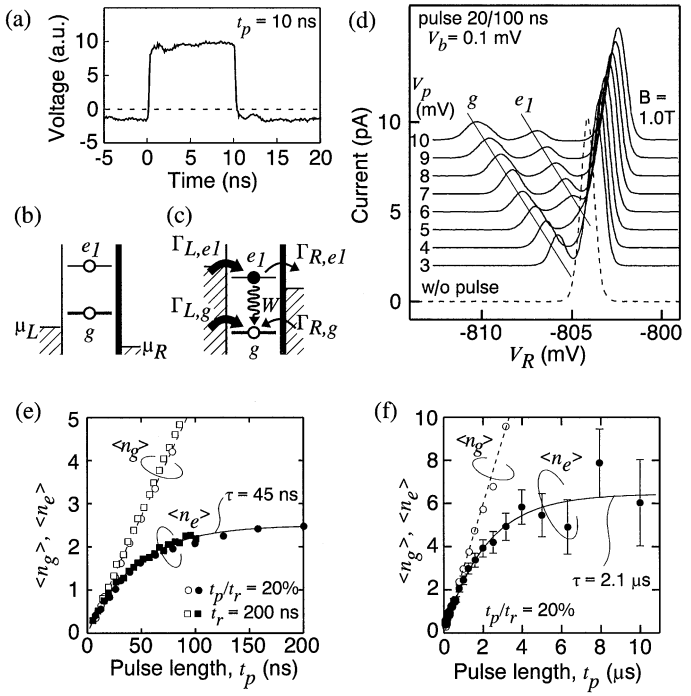

Fig. 2. (a) Typical pulse waveform. Signal reflected back from the gate electrode (no termination) is indicated. (b) and (c) Schematic energy diagrams. (b) is the situation just before the pulse is applied (steady state), and (c) is during the pulse. (d) Pulse-excited current measured at $V_b = 0.1$ mV. Each line is shifted for clarity. (e) and (f) Average number of tunneling electrons per pulse period through the GS ($\langle n_g \rangle$, open symbols) and through an ES ($\langle n_e \rangle$, filled symbols). Conditions: (e) is at $B = 1.1$ T for the $N+1$ electron state ($\Gamma_{R,g} = 26$ MHz, $\Gamma_{R,e} = 100$ MHz, $\Gamma_L/\Gamma_R \sim 15$) and (f) is at $B = 1.35$ T for the N electron state ($\Gamma_{R,g} = 1.1$ MHz, $\Gamma_{R,e} = 4.2$ MHz, $\Gamma_L/\Gamma_R \sim 300$).

barriers. For equilibrium transport $\langle n_g \rangle$ is linearly dependent on pulse length, t_p. The slope gives the tunneling rate, $\Gamma_{R,g}$, which is also the same as that obtained from DC measurements. Non-equilibrium transport $\langle n_e \rangle$ exhibits saturation behavior, which can be fitted well to a single exponential function, $\sim (1 - e^{t/\tau})$ (solid line). The decay time, τ, is 45 ns in Fig. 2(e), and a longer decay time of 2.1 μs is obtained from Fig. 2(f).

The decay time of the non-equilibrium transport depends on the energy relaxation rate, W. We can relate them from the non-equilibrium rate equations

$$\frac{d}{dt}\rho_{e1} = \Gamma_{L,e1}(1 - \rho_{e1} - \rho_g) - \Gamma_{R,e1}\rho_{e1} - W\rho_{e1},$$

$$\frac{d}{dt}\rho_g = (\Gamma_{R,g} + \Gamma_{L,g})(1 - \rho_{e1} - \rho_g) + W\rho_{e1}, \qquad (6)$$

by taking account of all the processes described in Fig. 2(c). Considering the initial condition, $\rho_g = \rho_{e1} = 0$ at $t = 0$, we obtain $\rho_{e1}(t) = A(1 - e^{-Ft})e^{-Dt}$. Assuming $\Gamma_L \gg \Gamma_R$ and $W < \Gamma_{L,e1} + \Gamma_{L,g}$ (valid for the visible current), $A \simeq \Gamma_{L,e1}/\Gamma_{L,e1} + \Gamma_{L,g}$ is the injection efficiency into the ES. The filling rate, $F \simeq \Gamma_{L,g} + \Gamma_{L,e1}$, is so large (> 1 GHz) that $e^{-Ft} \sim 0$ in our time domain. The decay rate,

$$D = W + \Gamma_{R,e1}(1 - A), \qquad (7)$$

contains information about W. The number of tunneling electrons, $\langle n_e \rangle$, can be written as

$$\langle n_e \rangle \simeq \int \Gamma_{R,e1}\rho_{e1}\,dt = A\Gamma_{R,e1}(1 - e^{-Dt})/D, \qquad (8)$$

which can be compared with the experimental data. Therefore, the relaxation rate W can be

estimated from the decay rate, $D = \tau^{-1}$, by using Eq. (7).

We can experimentally derive the tunneling rates, $\Gamma_{R,g}$ and $\Gamma_{R,e1}$ from the DC measurement, but $\Gamma_{L,e1}/\Gamma_{L,g} = \Gamma_{R,e1}/\Gamma_{R,g}$ must be assumed in order to obtain A. We obtained $\Gamma_{R,e1}(1-A) = 21$ MHz and $\tau^{-1} = 22$ MHz for the data in Fig. 2(e), and $\Gamma_{R,e1}(1-A) = 0.9$ MHz and $\tau^{-1} = 0.5$ MHz for the data in Fig. 2(f). Therefore, W is effectively zero, or much smaller than the observed τ^{-1}. This is true for all the ESs that appear in the pulse-excited current. The decay rate is always dominated by the tunneling rate, and the relaxation time is much longer than a few μsec for some ESs.

The non-equilibrium current is obtained only for specific ESs in the dot. The second ES that appears as a current step seen at $\mu_R = E_{e2}$ in negative bias of Fig. 1(b), does not appear in the pulse-excited current nor in the DC current at positive bias. Non-equilibrium current cannot be detected for our experimental set up, if the relaxation time is shorter than a few ns.

The short relaxation time can be easily understood by the electron–phonon interaction (typically less than 1 ns) [6,4]. By contrast, the long relaxation time (much longer than a few μs) is more than three orders of magnitude longer than that. If the ES and GS have different total spins, the relaxation involves a spin-flip and the rate is expected to be extremely small [5]. Spin-conservation during the relaxation is most likely in the quantum dot.

For the approximately ten ESs in a quantum dot that we investigated, the pulse-excited measurement and positively biased current measurement (discussed in the previous section) were qualitatively identical. The ES that appeared in the pulse current also appeared in positive DC current, and vice versa.

4. Magnetic field dependence

The magnetic field dependence of (a) $-\mathrm{d}I/\mathrm{d}V_R$ at a negative V_b, (b) $\mathrm{d}I/\mathrm{d}V_R$ at a positive V_b, and (c) pulse-excited current, I, is plotted in Fig. 3. All the ESs in the transport window are resolved as peaks in Fig. 3(a). The complicated magnetic field dependence is a result of crossings or anti-crossings among different energy states. For example, the ESs, e_1 and e_2, show anti-crossing behavior at $B_0 \sim 1.29$ T (indicated by a circle). The peak amplitudes and B dependence of their energies, or characteristics of the states, are exchanged at this magnetic field. The energy diagram around this crossing is shown schematically in Fig. 3(d) disregarding the energy splitting of the anti-crossing; e.g., α is the first ES at $B > B_0$ and the second ES at $B < B_0$. Only the state α is seen in both the positively biased current and the pulse-excited current. Other ESs including the state β are not detected, and thus their relaxation time is very short.

We measured the pulse-length dependence around the level crossing. Fig. 3(e) shows the ratio of the non-equilibrium current through the ES α and the equilibrium current through the GS, $\langle n_e\rangle/\langle n_g\rangle$. From Eq. (8), the ratio should be $\langle n_e\rangle/\langle n_g\rangle = C(1-\mathrm{e}^{-Dt})/Dt$, where $C = \Gamma_{L,e}\Gamma_{R,e}/(\Gamma_{L,e}+\Gamma_{L,g})\Gamma_{R,g}$ is usually about one. The decay rate D of the non-equilibrium current through the state α at $B > B_0$ differs significantly from that at $B < B_0$. We need two components to fit the data,

$$\frac{\langle n_e\rangle}{\langle n_g\rangle} = C_l\frac{1-\mathrm{e}^{-D_l t}}{D_l t} + C_s\frac{1-\mathrm{e}^{-D_s t}}{D_s t}, \tag{9}$$

where C_l and D_l are for the long-lived part and C_s and D_s are for the short-lived part. We kept $C_l + C_s$ constant for simplicity. D_l is comparable to $\Gamma_{R,e}(1-A)$, which is 0.3–1 MHz from the DC characteristics, and the actual relaxation time is much longer than a few μs. By contrast, $D_s \sim 300$ MHz of the short-lived part is much larger than $\Gamma_{R,e}(1-A)$, and this is the only occasion where we were able to determine the actual relaxation time of the excited state. The relaxation time, about 3 ns, is within the regime predicted by the electron–phonon interaction [4]. The relaxation rates, D_l and D_s, do not change, but the amplitude, C_l and C_s, change at the crossing. We observed no long-lived part for the magnetic field $B < 1.2$ T. The ES α lifetime is significantly reduced by the existence of the lower lying ES β at $B < B_0$.

We can speculate the energy relaxation process as shown in Fig. 3(d). Even though the relaxation from α to g is prohibited ($W_{g\alpha} \sim 0$), energy

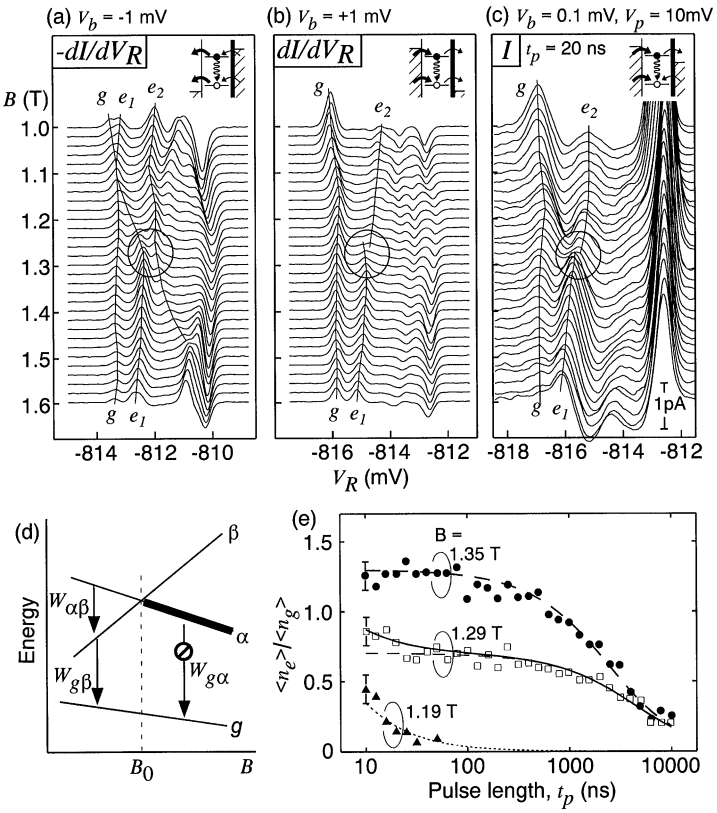

Fig. 3. (a), (b) and (c) Waterfall plots of (a) $-\mathrm{d}I/\mathrm{d}V_\mathrm{R}$ at $V_\mathrm{b} = -1$ mV, (b) $\mathrm{d}I/\mathrm{d}V_\mathrm{R}$ at $V_\mathrm{b} = +1$ mV, and (c) pulse-excited current, I, measured at $t_\mathrm{p}/t_\mathrm{r} = 20$ ns/100 ns. The magnetic field is varied from 1 to 1.6 T in steps of 0.02 T. The solid lines are guides for the eye for the ground state, g, and the first and second excited states, e_1 and e_2, respectively. Circles indicate where e_1 and e_2 cross (anti-cross) each other. Each inset shows the schematic energy diagram of the transport. (d) Schematic energy diagram of ground state, g, excited states, α and β. The thick line (α at $B > B_0$) is where the relaxation time is very long. (d) Pulse length dependence of $\langle n_\mathrm{e}\rangle/\langle n_\mathrm{g}\rangle$. The dotted and dashed lines are short and long relaxation part, respectively. The solid lines are sum of them to fit the data. The fitting parameters are $C_\mathrm{l} = 1.3$ and $D_\mathrm{l} = 0.7$ MHz for $B = 1.35$ T, $C_\mathrm{l} = 0.7$, $D_\mathrm{l} = 0.4$ MHz, $C_\mathrm{s} = 0.6$, $D_\mathrm{s} = 330$ MHz for $B = 1.29$ T, and $C_\mathrm{s} = 1.3$, $D_\mathrm{s} = 330$ MHz for $B = 1.19$ T.

relaxation from α to β can suppress the non-equilibrium transport through α. In this case, D_s is the relaxation rate $W_{\alpha\beta}$. The spin conservation model, in which the relaxation from the state i of total spin S_i to the state j of total spin S_j is blocked if $S_\mathrm{i} \neq S_\mathrm{j}$, gives a contradiction to our observation. According to the three level model described in Fig. 3(d), $S_\alpha \neq S_\mathrm{g}$ is necessary for a long-lived state α, and $S_\alpha = S_\beta$ and $S_\beta = S_\mathrm{g}$ are expected for the short relaxation. But this is obviously self-contradictory. The signal from ES β at $B < B_0$ might be too small to see the long relaxation time, because the ES β have a smaller tunneling rate than other states. We need further measurements to clear this point.

5. Summary

In summary, we have estimated the energy relaxation rate from an ES to a GS by means of DC current and pulse-excited current measurements. Although the relaxation is either too fast or too slow to allow the relaxation time to be estimated by our technique, a significantly different relaxation time can be explained by the spin-conservation

model. We also discussed a complicated situation where two ESs cross each other.

References

[1] L.P. Kouwenhoven et al., in: L.L. Sohn, L.P. Kouwenhoven, G. Schön (Eds.), Mesoscopic Electron Transport, NATO ASI Series E 345, pp. 105–214.
[2] L.P. Kouwenhoven et al., Science 278 (1997) 1788.
[3] S. Sasaki et al., Nature 405 (2000) 764.
[4] U. Bockelmann, Phys. Rev. B 50 (1994) 17271.
[5] A.V. Kaetskii, Yu.V. Nazarov, Phys. Rev. B 61 (2000) 12639, cond-mat/0003513.
[6] O. Agam et al., Phys. Rev. Lett. 78 (1997) 1956.
[7] T. Fujisawa et al., Science 282 (1998) 932.
[8] T. Fujisawa et al., Phys. Rev. Lett. B 63 (2001) 081304(R).
[9] T.H. Oosterkamp et al., Nature 395 (1998) 873.